Carbohydrate Polymers 88 (2012) 931–938

Contents lists available at SciVerse ScienceDirect

Carbohydrate Polymers

journal homepage: www.elsevier.com/locate/carbpol

Radiation synthesis and Cr(VI) removal of cellulose microsphere adsorbent

Youwei Zhang [a], Ling Xu [b], Long Zhao [c], Jing Peng [a], Cancan Li [a], Jiuqiang Li [a], Maolin Zhai [a,*]

[a] Beijing National Laboratory for Molecular Sciences, Department of Applied Chemistry and the Key Laboratory of Polymer Chemistry and Physics of the Ministry of Education, College of Chemistry and Molecular Engineering, Peking University, Beijing 100871, China
[b] Department of Energy and Resources Engineering, College of Engineering, Peking University, Beijing 100871, China
[c] School of Nuclear Science and Engineering, Shanghai Jiao Tong University, Shanghai 200240, China

ARTICLE INFO

Article history:
Received 9 December 2011
Received in revised form 8 January 2012
Accepted 14 January 2012
Available online 23 January 2012

Keywords:
Cellulose microsphere
Radiation grafting
Styrene
Adsorbent
Cr(VI)

ABSTRACT

A novel cellulose-based adsorbent was prepared by radiation-induced grafting of styrene onto the surface of cellulose microspheres, followed by acetylation and amination processes. The grafting yield was adjusted by the total absorbed dose, dose rate and the concentration of styrene. The structure of the adsorbent was characterized by micro-FTIR, XPS and SEM. The adsorption of Cr(VI) ions has been investigated as a function of contact time, adsorbent feed, pH, Cr(VI) and NaCl concentration. It was found that adsorption equilibrium could be achieved within 30 min for initial Cr(VI) of 100 mg L^{-1}. The adsorption kinetics was well described by the pseudo-second order model equation, and the adsorption isotherm was better fitted by the Langmuir mode. The maximum theoretical Cr(VI) uptake of the adsorbent was 123.4 mg g^{-1}. The influence of NaCl concentration on Cr(VI) uptake and XPS analysis revealed that Cr(VI) ions were adsorbed through ion-exchange mechanism.

1. Introduction

Water pollution due to toxic heavy metal ions has been attracting more and more attention in the past decades because heavy metal ions are potentially hazardous to human health and ecosystem even in minute quantities (Zhang, Gao, Zhai, Liu, & Gao, 2008). Chromium is a typical heavy metal which has been used extensively in industries such as electroplating, metal finishing, pigments and leather tanning (Xing, Zhang, Ju, & Yang, 2006). It is commonly found in two oxidation states; Cr(VI) and Cr(III). Cr(VI) is known to be highly mobile in soil and aquatic system, and hazardous to the biological systems and human health (Xu, Gao, et al., 2011). Therefore, the US Environmental Protection Agency (EPA) has set a maximum contaminant level of 0.05 mg L^{-1} for Cr(VI) in potable water (Park, Park, Yun, & Kim, 2008).

Different methods such as membrane separation, precipitation and solvent extraction have been used for the removal of heavy metal ions from wastewater (Futalan et al., 2011; Tian et al., 2011). Among these techniques, ion exchange is the most effective method owing to its regeneration, high efficiency and low cost (Zhao, Sun, Zhao, Xu, & Zhai, 2011). Several studies have been reported on metal ions adsorption by fiber (Xiong & Yao, 2009), membrane (Takase & Katoh, 1995) and powder adsorbents (Qiu et al., 2009). However, these adsorbents were not suitable for column packing due to their poor mechanical properties.

Recently, microsphere adsorbents have attracted much interest because of their large surface area, low cost, ease of operation and high mechanical stability (Hou, Wang, Gao, & Yang, 2008). Cellulose is the most abundant and renewable biopolymer in nature. It possesses very attractive advantages including cost-effective, biodegradability, non-toxicity, thermal and chemical stability. It has been considered as one of the economical promising materials for the preparation of adsorbents (Siroky, Blackburn, Bechtold, Taylor, & White, 2011). However, the heavy metal ions adsorption capacity of unmodified cellulose is very low. It was reported that some cellulose-based biosorbents exhibited good adsorption capacity for heavy metal ions when they possess functional groups such as carboxyl groups (Park, Park, Yun, & Jo, 2005). Therefore, it is possible that the functionalization of cellulose can be carried out to get an efficient adsorbent for removing heavy metal ions.

Radiation-induced grafting technique has exhibited obvious advantages over traditional methods since the composition and properties of the resulting adsorbents can be easily controlled by applying appropriate grafting conditions. Moreover, radiation-induced grafted polymer adsorbents fulfill most of the desired criteria such as high adsorption capacity, fast uptake and regeneration (Kumar, Bhardwaj, Jamdar, Goel, & Sabharwal, 2006). Therefore, the technique has been widely used to synthesis ion exchange adsorbents for the removal of heavy metal ions from wastewater (Zhao & Mitomo, 2008). However, to the best of our

Abbreviations: CPS, styrene grafted cellulose microspheres; CACPS, chloroacetylated CPS; AMCPS, aminated CACPS; AEM, anion exchange microspheres.

* Corresponding author. Tel.: +86 10 62753794; fax: +86 10 62753794.
E-mail address: mlzhai@pku.edu.cn (M. Zhai).

0144-8617/$ – see front matter © 2012 Elsevier Ltd. All rights reserved.
doi:10.1016/j.carbpol.2012.01.040

knowledge, ion exchanger based on cellulose microsphere, formed by radiation-induced grafting technique, has not yet been described in the literature.

The aim of this work is to develop a novel cellulose-based ion exchange adsorbent for removing heavy metal ions. The adsorbent was prepared by radiation-induced grafting of styrene onto the surface of cellulose microspheres, followed by acetylation and amination processes. The effects of adsorbed dose, dose rate and monomer concentration on the grafting yield were investigated. Parameters including contact time, adsorbent feed, solution pH, Cr(VI) and NaCl concentration that might influence the adsorption efficiency, were also discussed in detail.

2. Experimental

2.1. Materials

Cellulose microspheres (Average particle size ~240 μm) were obtained from Asahi Kasei Chemicals Corporation (Japan). Styrene (St) (purity > 99%) was purchased from Acros Organics (Morris Plains, NJ). Chloroacetic chloride and Potassium dichromate ($K_2Cr_2O_7$) were obtained from Sinopharm Chemical Reagent Co., Ltd. Diethylamine was supplied by Shantou Xi Long Chemical Factory. Methanol and toluene were purchased from Beijing Tong Guang Fine Chemicals Company. All reagents were analytical-grade chemicals and were used as received without further purification.

2.2. Preparation of the adsorbent

The preparation procedure of the adsorbent is illustrated in Scheme 1. The simultaneous radiation grafting method was used.

2.2.1. Radiation-induced graft polymerization

Cellulose microspheres were completely immersed in St/methanol solution and left for 24 h to facilitate the swelling of cellulose microspheres. After getting rid of oxygen by nitrogen flow for 15 min, the sealed glass tubes were then irradiated in a ^{60}Co γ-chamber for various doses, dose rates and St concentrations. After irradiation, the residual monomer and homopolymer attached to the grafted samples were removed by 24 h extraction in a Soxhlet extractor with toluene as extractant. The samples were then dried in a vacuum oven at 50 °C for 24 h and weighted. The grafting yield (GY) was determined by the percentage increase in weight as follows:

$$\mathrm{GY}\ (\%) = \frac{W_g - W_0}{W_0} \times 100 \quad (1)$$

where W_0 and W_g are the weights of the initial and grafted cellulose microspheres, respectively.

St grafted cellulose microspheres (CPS) with 52% and 100% GY were prepared and used as the substrates for further chemical modification.

2.2.2. Chloroacetylation of CPS

CPS (5.0 g) was first acylated by refluxing with chloroacetyl chloride (5.5 g) and anhydrous aluminium chloride (7.0 g) in dichloromethane (50 mL) at room temperature for 7 h with constant stirring. The chloroacetylated samples (CACPS) were washed with THF, hydrochloric acid (3%), deionized water and methanol, respectively. The samples were then dried in a vacuum oven at 50 °C for 24 h.

2.2.3. Amination of CACPS

An appropriate amount of CACPS (4.0 g) was allowed to swell in THF solution (40 mL) overnight. Diethylamine (18 g) and sodium bicarbonate (1.6 g) were added to the swollen samples in a three-neck flask fitted with condenser. The amination reaction of CACPS was carried out at 70 °C (2 h) with constant stirring. After the reaction, the aminated CACPS (AMCPS) were purified by washing with deionized water, and then dried in a vacuum oven at 50 °C for 24 h.

2.2.4. Preparation of anion exchange microspheres (AEM)

The preparation of AEM was carried out by immersing AMCPS in 1 mol L^{-1} HCl solution for 24 h. The resulting AEM was dried in a vacuum oven at 50 °C for 24 h. Two kinds of AEM were synthesized and used for further batch experiments. GY of St for AEM-I and AEM-II were 52% and 100%, respectively.

2.3. Characterization of AEM

2.3.1. Micro-FTIR analysis

Micro-FTIR analysis of the original cellulose microsphere, CPS, CACPS, AMCPS and AEM-I were performed in a Nicolet (Magna-IR 750) spectrometer. The spectra were measured in the absorbance mode in range of 4000–600 cm^{-1}.

2.3.2. XPS analysis

The X-ray photoelectron spectroscopy (XPS) analysis was performed with an AXIS-Ultra instrument from Kratos Analytical using monochromatic Al Kα radiation (225 W, 15 mA, 15 kV) and low energy electron flooding for charge compensation. To compensate for surface charges effects, binding energies (BE) were calibrated using C1s hydrocarbon peak at a BE of 284.80 eV. The data were

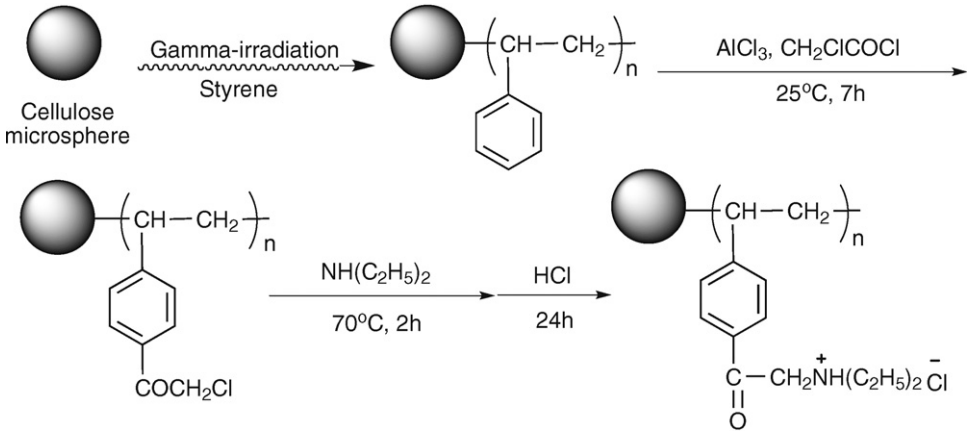

Scheme 1. Synthetic route of cellulose microsphere adsorbent.

converted into VAMAS file format and imported into CASA XPS software package for manipulation and curve fitting.

2.3.3. Morphology observation of AEM

Dried AEM was immersed directly in solution with different pH at room temperature to equilibrium (24 h). The swollen equilibrium AEM was frozen to −70 °C and then freeze-dried under a vacuum until all water was sublimed. Morphology of the surface of freeze-dried samples was observed by scanning electron microscope (SEM) (Hitachi S4700).

2.3.4. Ion exchange capacity (IEC) and nitrogen content

Ion exchange capacity (*IEC*) was determined by titration. An appropriate amount of AMCPS were immersed in a 0.05 mol L^{-1} HCl solution at room temperature for 24 h with constant stirring. Then the solution was back titrated with 0.05 mol L^{-1} NaOH to neutral. The *IEC* (mmol g^{-1}) was calculated by the equation as follows:

$$IEC = \frac{M_{HCl} - M_{NaOH}}{W} \quad (2)$$

where M_{HCl} is the mole of HCl, M_{NaOH} is that of the required NaOH, W is the weight of the adsorbent.

The nitrogen content of AEM was determined with an Elemental Analyzer (Elementar Vario EL, Germany).

2.4. Adsorption of Cr (VI) onto AEM

The standard stock solution of Cr (VI) (1000 ppm) was obtained by dissolving $K_2Cr_2O_7$ in distilled water. Certain amount of HCl was added in order to stabilize Cr(VI) ions in the solution. The concentration of HCl in the stock solution was 0.02 mg L^{-1}. This solution was then diluted with distilled water to desired concentrations.

Kinetics study was carried out as follows: 0.050 g adsorbent was added to 250 mL beaker containing 50 mL Cr(VI) solution (100 ppm). The beaker was then placed in an incubator shaker (140 rpm) at room temperature. Cr(VI) concentration was measured by UV-Visible Spectrophotometer (UV-3010, HITACHI) at 540 nm by 1, 5-diphenyl carbamide method (Samani, Borghei, Olad, & Chaichi, 2010). Cr(VI) uptake was calculated as

$$\text{Cr(VI)} \quad \text{uptake} = (C_0 - C_e) \times \frac{V}{m} \quad (3)$$

where C_0 and C_e are the concentrations of Cr(VI) before and after adsorption, respectively; V is the volume of the Cr(VI) solution and m is the weight of dry adsorbent.

The influence of pH, adsorbent feed, Cr(VI) and NaCl concentration on Cr(VI) uptake was also conducted using a very similar procedure. pH was adjusted with 1 mol L^{-1} HCl or 1 mol L^{-1} NaOH. All values were measured in duplicate with uncertainty within 3%.

2.5. Desorption of Cr(VI)

Desorption behavior of Cr(VI) was studied as follows: immersing AEM-II which had fully adsorbed Cr(VI) ions into 1 mol L^{-1} NaCl solution for 24 h, then washed with distilled water and dried in a vacuum oven at 50 °C (24 h) for XPS analysis.

3. Results and discussion

3.1. Preparation of AEM

The effect of absorbed dose on the GY of St onto cellulose microspheres was investigated (Fig. 1A). The GY increases obviously with increasing absorbed dose. It is reported that the process of ^{60}Co γ irradiation graft polymerization is mainly a free radical mechanism,

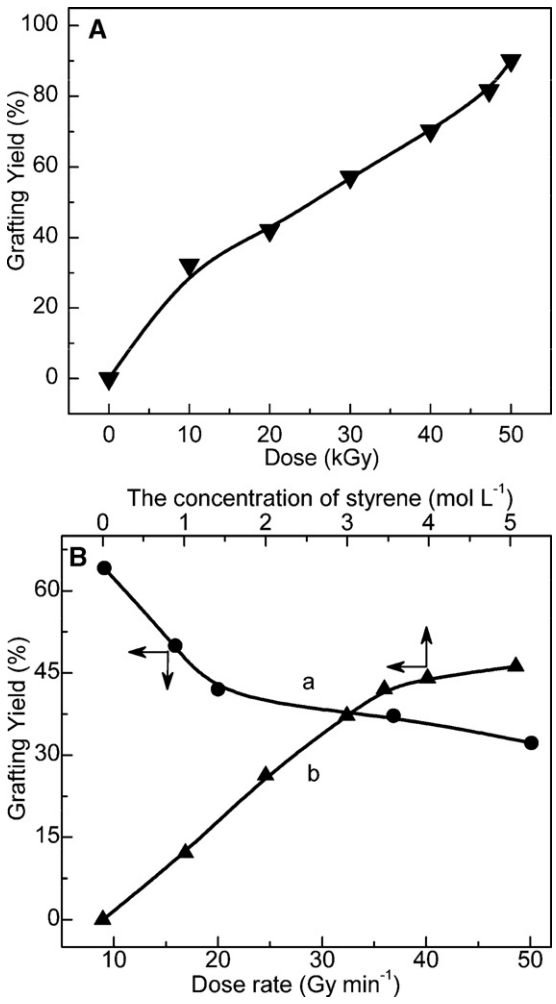

Fig. 1. Effect of dose on the GY of St at dose rate of 20 Gy min^{-1} (St concentration: 4 mol L^{-1}) (A); Effects of dose rate (a) and monomer concentration (b) on the GY of St at room temperature (dose: 20 kGy) (B).

and the grafting polymerization is controlled by the total amount of free radicals formed in both the substrates and monomer solution (Qiu et al., 2007). The total amount of free radicals formed on the substrates as well as in monomer solution in the system increase with increasing absorbed dose.

The effect of the dose rate on the GY of St onto cellulose microspheres is shown in Fig. 1B (a). The increase in the dose rate during irradiation resulted in a decrease in the GY. At a high dose rate, the radicals formed in the substrates tend to decay by recombination faster than at lower dose rate. Therefore, the grafting process is inhibited on account of the decreasing amount of radical sites in the substrates. Also, at higher dose rate, the grafted polystyrene chains are subjected to faster termination, and consequently the GY of St decreases, which is in accordance with the result that reported in reference (Cardona, George, Hill, Rasoul, & Maeji, 2002).

The concentration of monomer during radiation-induced grafting polymerization also affects the kinetic parameters of this process. Fig. 1B (b) shows the effect of St concentration on the GY. The GY increases linearly with St concentration from 0 to 4 mol L^{-1} and then levels off beyond 4 mol L^{-1}. Since methanol is a nonsolvent for polystyrene moieties, the growing chains in the polymerization are immobilized and the termination reaction is inhibited at a low monomer concentration, resulting in an increasing GY (Nho, Chen, & Jin, 1999). As monomer concentration increases, the rate of propagation reaction is overcome by the greatly increased termination

rate of monomer radicals reacting between monomer radicals and growing polystyrene chains grafted onto the substrates. In addition, the GY also depends on the diffusibility of monomer through grafting chains. As monomer concentration increases, the diffusibility of monomer decreases with the increase in the viscosity of grafting medium due to homopolymerization. This subsequently results in lower diffusion of monomer to the substrates, and hence limits the rapid growth of GY.

Chloroacetylation and amination of CPS resulted in the formation of ammonium salt groups on the surface of substrates, which would probably result in high *IEC* and Cr(VI) uptake.

3.2. Characterizations of the adsorbent

3.2.1. Micro-FTIR analysis

Micro-FTIR spectra have been used as a useful tool to verify the presence of certain functional groups in modifications of materials. The micro-FTIR spectra of the cellulose microsphere, CPS, CACPS and AMCPS in the range of 4000–600 cm^{-1} are shown in Fig. 2A. The GY of St grafted onto cellulose microspheres is 52%. The broad and strong bands around 3370 cm^{-1} are due to abundant hydrogen bonded hydroxyl group (—OH) of cellulose (Seppala et al., 2011). In cellulose microspheres, strong absorption bands at 1050 cm^{-1} are assigned to the stretching vibration of cellulose ring C—O. The absorption bands at 1370 and 2900 cm^{-1} represent the stretching and bending vibration of cellulose ring C—H, respectively. Grafting of styrene is verified by the characteristic absorption bands of aromatic ring at 1490 and 1600 cm^{-1}, corresponding to aromatic C=C in-plane stretching vibration. Strong absorption bands at 696 and 760 cm^{-1} are due to the aromatic C—H deformation of substituted benzene ring (Zhang & McCormick, 1997). The spectrum also shows the characteristic absorption bands of aromatic ring at 3030 cm^{-1} (=C—H stretching vibration). Compared with the spectrum of CPS, strong bands appear in CACPS at 1210 and 1690 cm^{-1}, corresponding to the rocking of $—CH_2—Cl$ and the stretching of the carbonyl group, which indicates successful acetylation of CPS (Qu, Zhou, Wei, Su, & Ma, 2008). The amination of CACPS is confirmed by the presence of sharp absorption bands at 1380 and 2970 cm^{-1}, which are assigned to the rocking and stretching vibration of $—CH_3$ introduced by amination. It is obvious that the $—CH_2—Cl$ peak gets weakened on account of the substitution of chloromethyl groups by amination. The spectrum of the AEM-I is the same as that of AMCPS (data not shown).

3.2.2. XPS analysis

XPS is known as a powerful tool to analyze the elemental composition of the compounds. Fig. 2B shows XPS wide scan spectra of CPS (a), CACPS (b) and AEM-I (c). All compounds show two primary characteristic peaks corresponding to C_{1s} and O_{1s} at BE of 284.8 and 533.3 eV, respectively. The acetylated of CPS is confirmed by the presence of the sharp peaks corresponding to Cl_{2s} and Cl_{2p} at BE of 269.8 and 201.8 eV, respectively. A sharp peak appears after amination at BE of 400.1 eV, which is in agreement with typical N (1s) binding energies, revealing that AEM is prepared by amination with diethylamine.

The N 1s peak is curve-fitted with two peak components (Fig. 2C). One appears at BE of 399.4 eV which is due to $—N(C_2H_5)_2$ groups. The other having higher BE at 401.7 eV can be regarded as a signal from the positively charged nitrogen atoms of $—NH^+(C_2H_5)_2$ groups (Vallapa et al., 2011).

3.2.3. Morphology observation of AEM

The SEM micrographs of AEM-II before and after swelling experiment in different pH are given in Fig. 3. The structure of AEM is nonporous before swelling experiment (Fig. 3a and b). However,

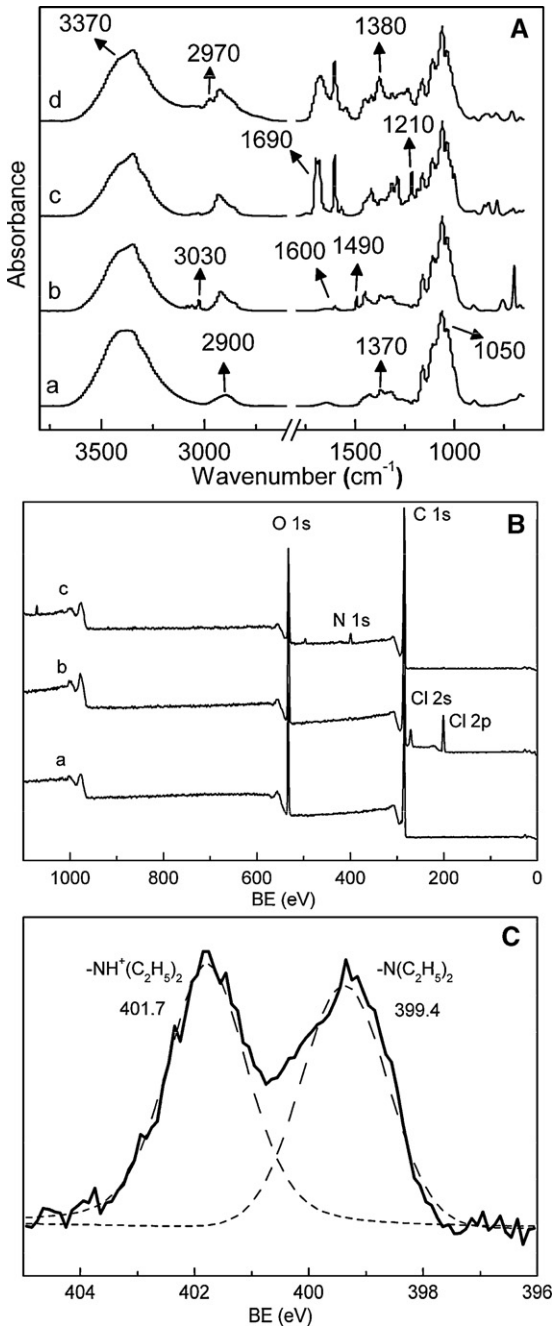

Fig. 2. FITR spectra of Cellulose (a), CPS (52% GY) (b), CACPS (c) and AMCPS (d) (A); XPS wide-scan spectra of CPS (52% GY) (a), CACPS (b) and AEM-I (c) (B); N 1s curve-fitting of AEM-I (C).

after immersed in acidic solution (pH = 1.34, 3.75 and 6.38), AEM reveals a porous structure and high surface area (Fig. 3c, d, and e). There are numerous $—N(C_2H_5)_2$ groups on the surface of AEM. When pH is less than 7, $—N(C_2H_5)_2$ groups are protonated to $—NH^+(C_2H_5)_2$ groups with the help of H^+. The electrostatic repulsion among the $—NH^+(C_2H_5)_2$ groups results in the increase in the mount and size of pores in acidic solution (Tan, Zhao, & Kang, 2006). While pH is more than 7, $—N(C_2H_5)_2$ groups are predominant, leading to the decrease in electrostatic repulsion among $—NH^+(C_2H_5)_2$ groups on the surface of AEM. Therefore, the amount and size of pores decrease (Fig. 3f). Because AEM possesses complex and porous surface texture and porosity in acidic solution, Cr(VI) ion can easily diffuse in and out. Therefore, the adsorbents

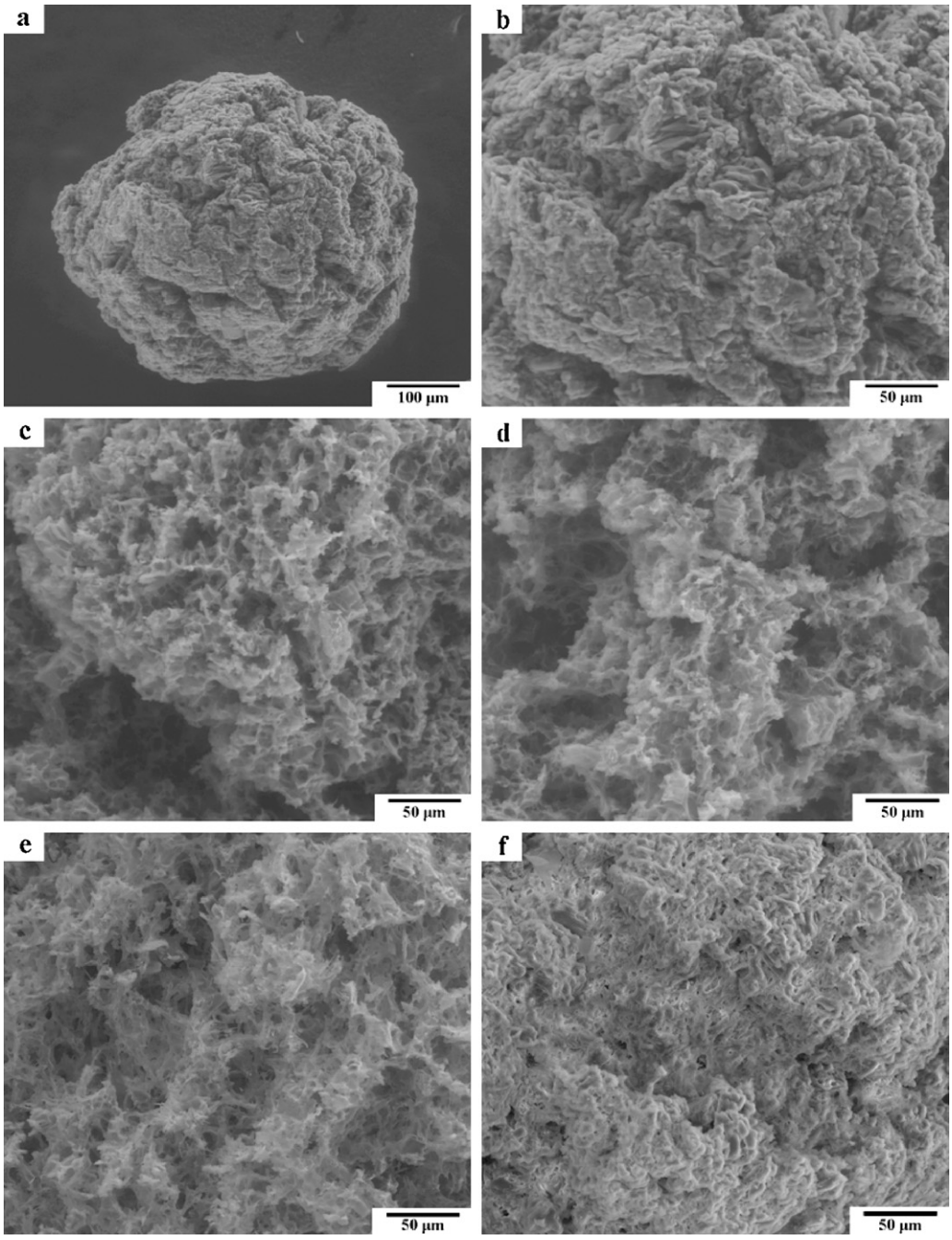

Fig. 3. SEM micrographs of AEM-II before (a, b) and after swelling experiment in different pH: (c) pH = 1.34; (d) pH = 3.75; (e) pH = 6.38; (f) pH = 10.72.

may have relative high adsorption capacity and fast adsorption kinetics.

3.3. Adsorption of Cr(VI)

3.3.1. The adsorption kinetics

The contact time to reach maximum adsorption is of great importance for studying the affinity of adsorbents to Cr(VI) ions. Therefore, the effect of contact time on the adsorption of Cr(VI) was studied and shown in Fig. 4A. The removal rate of Cr(VI) is initially rapid, but it gradually decreases with time until it reaches equilibrium at about 30 min. The experimental results indicate that the adsorbents (AEM-I and AEM-II) have rather rapid adsorption kinetics. In order to achieve the saturated adsorption, 40 min is chosen as the equilibrium time.

The mechanisms of adsorption processes were also investigated according to pseudo-first-order and pseudo-second-order kinetic equations which were given by Eqs. (4) and (5), respectively.

$$\log(q_e - q_t) = \log\ q_e - \frac{k_1}{2.303}t \tag{4}$$

$$\frac{t}{q_t} = \frac{1}{q_e}t + \frac{1}{k_2 q_e^2} \tag{5}$$

where q_t and q_e are the amount of Cr(VI) adsorbed ($mg\,g^{-1}$) at time t (min) and at equilibrium, respectively. k_1 is the rate constant of the pseudo-first-order adsorption process (min^{-1}), and k_2 is the rate constant for the pseudo-second-order model (Wang, Peng, Yang, Liu, & Hu, 2011). The parameters q_e, k_1, and k_2 are tabulated in Table 1. The correlation coefficients (R^2) for

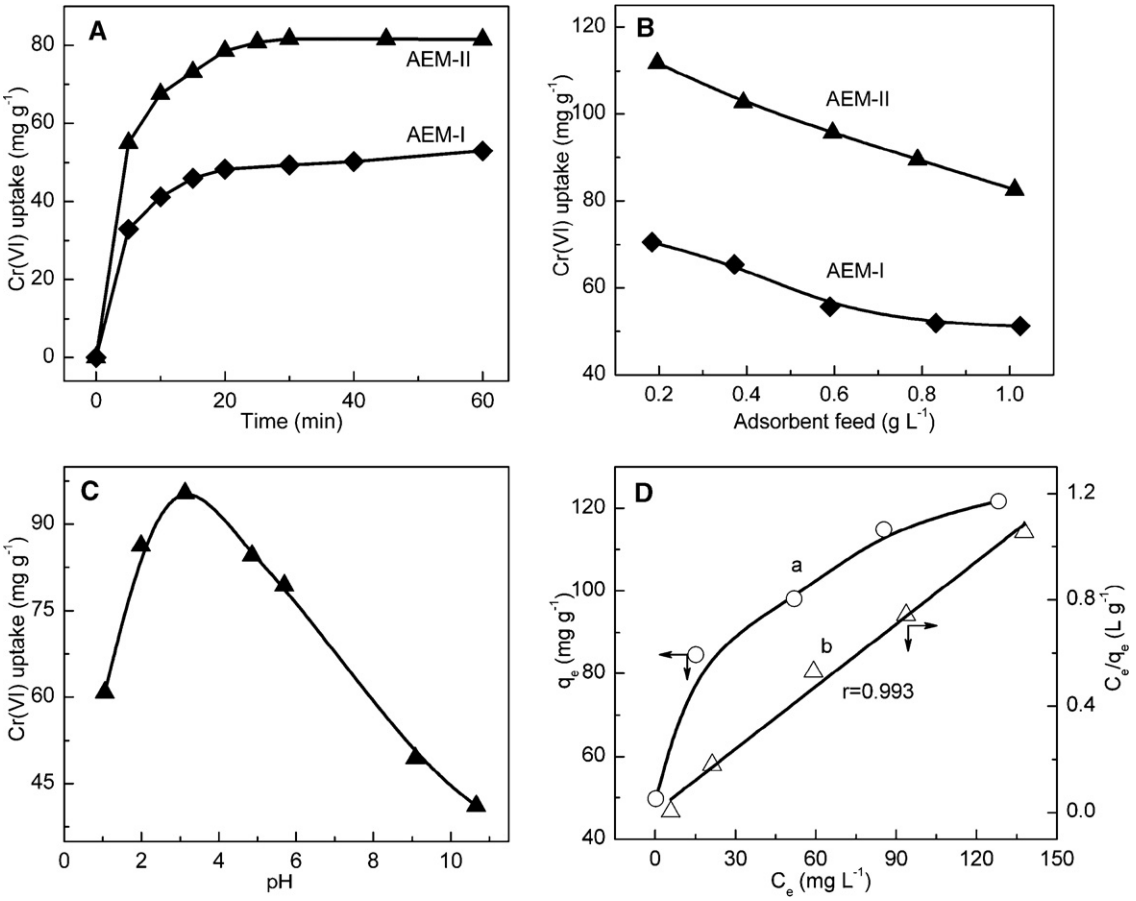

Fig. 4. Dynamics of Cr(VI) removal by AEM-II in 50 mL 100 mg L^{-1} solution (A); Effect of adsorbent feed on the adsorption of Cr(VI) in 50 mL 100 mg L^{-1} solution (stirring time: 40 min; pH: 4.68) (B); Effect of solution pH on the adsorption of Cr(VI) by AEM-II in 50 mL 100 mg L^{-1} solution (stirring time: 40 min; adsorbent feed: 1.0 g L^{-1}) (C); Experimental Cr(VI) adsorption on AEM-II (a) and Langmuir linear plot (b) (adsorbent feed: 1.0 g L^{-1}; stirring time: 40 min; pH: 4.68; V: 50 mL) (D).

the pseudo-second-order kinetic model are both 0.999, suggesting that pseudo-second-order model represents the present adsorption system, which implies that the adsorption is an ion exchange process (Xu, Zhao, Sun, Zhao, & Zhai, 2011).

3.3.2. IEC and Cr(VI) uptake

IEC is an indication of the content of ammonium salt groups in the adsorbent. High *IEC* of adsorbents shows higher amount of ammonium salt groups existed in the adsorbent. *IEC* of AEM-I and AEM-II are presented in Table 2. As expected, *IEC* of AEM increases with GY and nitrogen content. In addition, the Cr(VI) uptakes of AEM-I and AEM-II are 55.6 and 85.5 mg g^{-1}, while the *IEC* of AEM-I and AEM-II are 1.71 and 2.60 mmol g^{-1}. The Cr(VI) uptake is in the relative high level among all the modified and unmodified biosorbents reported in references (Owlad, Aroua, Daud, & Baroutian, 2009). In the control experiment, the original cellulose microsphere could not adsorb Cr(VI) (data not shown). High ion exchange capacity and Cr(VI) uptake of AEM can be attributed to the grafted functional groups, while the cellulose microspheres serve as the backbone of AEM. Besides, the average diameters of AEM-I and AEM-II are ~424 and ~489 μm, respectively, which is suitable for column packing in wastewater treatment.

3.3.3. Effect of adsorbent feed

The adsorbent feed is another important parameter in adsorption process of Cr(VI). The effect of adsorbent feed on the adsorption of Cr(VI) was studied (Fig. 4B). The adsorbent feed is in the range from 0.2 to 1.0 g L^{-1}. The adsorption capacity of Cr(VI) decreases with increasing adsorbent feed, which can be attributed to the fact that the amount of unsaturated adsorption sites increase with the increasing of adsorbent feed.

3.3.4. Effect of solution pH

Knowledge of the optimum pH is very important in the practical use since pH affects both the surface charge of adsorbent and the existing forms of adsorbates. The optimum range of pH for the maximum adsorption of Cr(VI) onto AEM-II was investigated (Fig. 4C). The maximal Cr(VI) uptake (95.4 mg g^{-1}) is obtained at pH 3.1. Cr(VI) uptake decreases by either raising or lowering the pH. However, even when the pH reaches 1.0 or 10.6, AEM-II still exhibits a sound Cr(VI) uptake of 60.7 and 44.1 mg g^{-1}, respectively.

Table 1
Pseudo-first-order and pseudo-second-order kinetic parameters for the adsorption of Cr(VI) on AEM-I and AEM-II.

Adsorbent	Pseudo-first-order			Pseudo-second-order		
	k_1 (min^{-1})	q_e (mg g^{-1})	R^2	k_2 (g mg^{-1} min^{-1})	q_e (mg g^{-1})	R^2
AEM-I	3.44	55.7	0.994	0.005	55.6	0.999
AEM-II	3.08	88.5	0.984	0.005	85.5	0.999

Table 2
Parameters of AEM-I and AEM-II.

Adsorbent	GY (%)	Diameter (μm)	Nitrogen content (%)	*IEC* (mmol g^{-1})	q_e (mg g^{-1})	q_m (mg g^{-1})
AEM-I	52	~424	2.6	1.71	55.6	69.5
AEM-II	100	~489	3.7	2.60	85.5	123.4

Therefore, this novel adsorbent can be applied in some extreme environment due to its high acidic and alkaline resistance.

Cr(VI) can exist in several stable forms in aqueous solution, but the relative abundance of them are dependent on solution pH and Cr(VI) concentration (Neagu, 2009). When pH is less than 1.0, $H_2Cr_2O_7$ are predominant, leading to the decrease in electrostatic attraction between adsorbent and Cr(VI) ions. As a result, the Cr(VI) uptake is low at pH 1.0. The decrease in the adsorption with the increase in pH from 7.0 to 12.0 may be attributed to the competition of OH^- and the deprotonation of the $-NH^+(C_2H_5)_2$ groups. Similar results have been reported in the literature (Qiu et al., 2009). The results also show that electrostatic attraction results in the adsorption at the pH from 1.0 to 6.0, while at higher or lower pH, other interaction such as the chelation interaction, hydrogen bonding and the weak van der Waals forces enhance the adsorption capacity (Ting & Deng, 2005).

3.3.5. *The isotherm of adsorption of Cr(VI) ions*

Adsorption isotherm can be used to investigate how Cr(VI) ions interact with the adsorbent. It is characterized by certain constants. The Langmuir isotherm model is often used to study the relationship between Cr(VI) uptake and the equilibrium concentration in solution and is effective for homogeneous and monolayer adsorption onto a surface with a finite number of identical sites (Zhai et al., 2009). It is defined as Eq. (6)

$$\frac{C_e}{q_e} = \frac{C_e}{q_m} + \frac{1}{K_L q_m} \quad (6)$$

where C_e (mg L^{-1}) is the equilibrium concentration of Cr(VI) in solution, q_m (mg g^{-1}) is the maximum adsorption at monolayer, q_e (mg g^{-1}) is the amount of Cr(VI) adsorbed by per gram adsorbent, K_L is Langmuir constant related to the affinity of binding sites, which is a measure of the energy of adsorption. The slope and the intercept of the linear plot of C_e/q_e versus C_e enable the constants of Langmuir adsorption isotherm to be determined.

The Langmuir plot of Cr(VI) adsorption onto AEM-II is shown in Fig. 4D. The linear correlation coefficient (r) is 0.993, which reveals that the adsorption well fit the Langmuir model. The isotherm constants q_m and K_L are calculated as 123.4 mg g^{-1} and 0.167 L g^{-1}, respectively. The q_m of AEM-I were also calculated as 69.5 mg g^{-1} (Table 2). The experimental Cr(VI) uptake is lower than the theoretical maximum adsorption capacity. It may be attributed to the incomplete contact of Cr(VI) and the adsorbent.

3.3.6. *Effect of NaCl concentration and adsorption mechanism*

The effect of NaCl concentration on the adsorption of Cr(VI) ions was investigated (Fig. 5A). The experiment was conducted with 1.0 g L^{-1} adsorbent in 100 mg L^{-1} Cr(VI) solution. Cr(VI) uptake decreases with the increase in NaCl concentration, which is mainly attributed to increasing competition of Cl^-. More Cl^- instead of Cr(VI) ions mainly interact with $-NH^+(C_2H_5)_2$ groups through electrostatic attraction. Besides, the addition of NaCl also results in a negative effect on the diffusion of Cr(VI) ions by restricting their mobility (El-Bayaa, Badawy, & AlKhalik, 2009).

To further investigate the mechanism of Cr(VI) adsorption, the XPS spectra of adsorbent are shown in Fig. 5B. After Cr(VI) adsorption, a typical peak at BE of ca. 579.1 eV corresponding to Cr_{2p} can be observed in XPS spectra. However, it is noticeable that the Cr_{2p} peak nearly disappears after desorption, while two new peaks at BE of

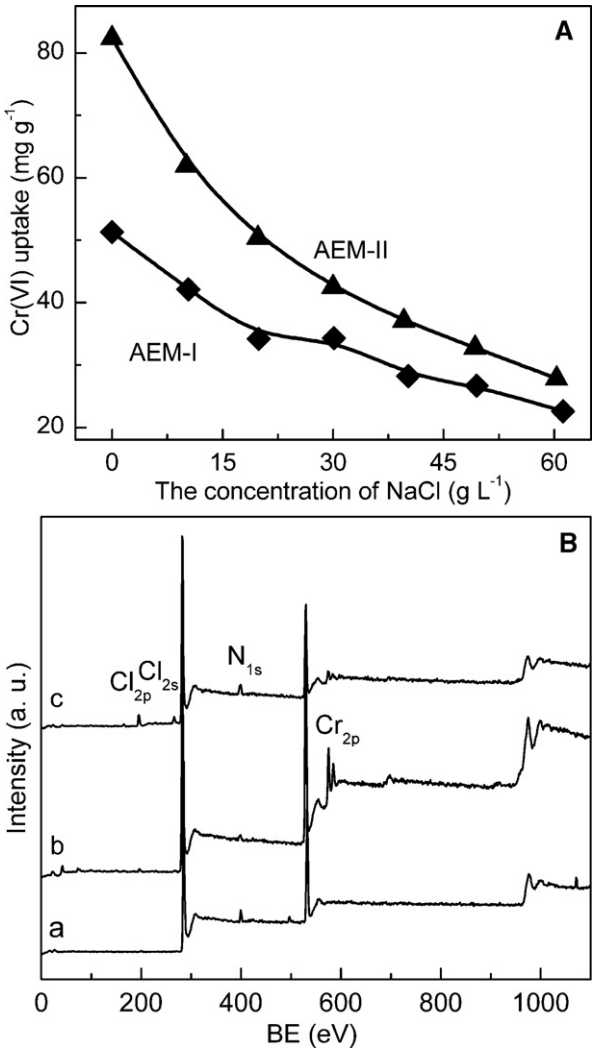

Fig. 5. Effect of NaCl concentration on the adsorption of Cr(VI) using 50 mL model solution of 100 mg L^{-1} (stirring time: 40 min; pH: 4.68) (A); XPS wide-scan spectra of AEM-II before (a), after (b) Cr(VI) adsorption and desorption (c) (B).

195.7 eV and 266.0 eV appear, which are in agreement with typical Cl_{2p} and Cl_{2s} binding energies. It can be concluded that the Cr(VI) ions are adsorbed onto the adsorbent through the ion exchange.

4. Conclusion

A novel anion-exchange cellulose-based microsphere for wastewater treatment was synthesized successfully by radiation grafting of styrene onto cellulose microsphere, followed by acetylation and amination processes. The structure of adsorbent was testified with FTIR and XPS analysis. The adsorbent possesses complex and porous surface texture in acidic solution. The adsorption equilibrium can be achieved with 30 min due to the strong electrostatic interaction between the adsorbent and $HCrO_4^-$. The optimum adsorption was observed at pH 3.1 for initial Cr(VI) concentration of 100 mg L^{-1}. The Cr(VI) adsorption followed pseudo-second order mode and decreased with increasing NaCl concentration suggesting

that the adsorption is a process of ion exchange. The adsorption experimental data fitted Langmuir isotherm with maximum theoretical Cr(VI) uptake of 123.4 mg g^{-1}. As a consequence, there is no doubt that the work has provided a new candidate of adsorbent for Cr(VI) removal in wastewater treatment.

References

Cardona, F., George, G. A., Hill, D. J. T., Rasoul, F., & Maeji, J. (2002). Copolymers obtained by the radiation-induced grafting of styrene onto poly(tetrafluoroethylene-co-perfluoropropylvinyl ether) substrates. 1. Preparation and structural investigation. *Macromolecules*, *35*(2), 355–364.

El-Bayaa, A. A., Badawy, N. A., & AlKhalik, E. A. (2009). Effect of ionic strength on the adsorption of copper and chromium ions by vermiculite pure clay mineral. *Journal of Hazardous Materials*, *170*(2–3), 1204–1209.

Futalan, C. M., Kan, C. C., Dalida, M. L., Hsien, K. J., Pascua, C., & Wan, M. W. (2011). Comparative and competitive adsorption of copper, lead, and nickel using chitosan immobilized on bentonite. *Carbohydrate Polymers*, *83*(2), 528–536.

Hou, X., Wang, X. K. K., Gao, B., & Yang, J. (2008). Preparation and characterization of porous polysucrose microspheres. *Carbohydrate Polymers*, *72*(2), 248–254.

Kumar, V., Bhardwaj, Y. K., Jamdar, S. N., Goel, N. K., & Sabharwal, S. (2006). Preparation of an anion-exchange adsorbent by the radiation-induced grafting of vinylbenzyltrimethylammonium chloride onto cotton cellulose and its application for protein adsorption. *Journal of Applied Polymer Science*, *102*(6), 5512–5521.

Neagu, V. (2009). Removal of Cr(VI) onto functionalized pyridine copolymer with amide groups. *Journal of Hazardous Materials*, *171*(1–3), 410–416.

Nho, Y. C., Chen, J., & Jin, J. H. (1999). Grafting polymerization of styrene onto preir-radiated polypropylene fabric. *Radiation Physics and Chemistry*, *54*(3), 317–322.

Owlad, M., Aroua, M. K., Daud, W. A. W., & Baroutian, S. (2009). Removal of hexavalent chromium-contaminated water and wastewater: A review. *Water, Air, and Soil Pollution*, *200*(1–4), 59–77.

Park, J. M., Park, D., Yun, Y. S., & Jo, J. H. (2005). Mechanism of hexavalent chromium removal by dead fungal biomass of Aspergillus niger. *Water Research*, *39*(4), 533–540.

Park, J. M., Park, D., Yun, Y. S., & Kim, J. Y. (2008). How to study Cr(VI) biosorption: Use of fermentation waste for detoxifying Cr(VI) in aqueous solution. *Chemical Engineering Journal*, *136*(2–3), 173–179.

Qiu, J. Y., Ni, H. F., Zhai, M. L., Peng, J., Zhou, H. H., Li, J. Q., et al. (2007). Radiation grafting of styrene and maleic anhydride onto PTFE membranes and sequent sulfonation for applications of vanadium redox battery. *Radiation Physics and Chemistry*, *76*(11–12), 1703–1707.

Qiu, J. Y., Wang, Z. Y., Li, H. B., Xu, L., Peng, J., Zhai, M. L., et al. (2009). Adsorption of Cr(VI) using silica-based adsorbent prepared by radiation-induced grafting. *Journal of Hazardous Materials*, *166*(1), 270–276.

Qu, J. B., Zhou, W. Q., Wei, W., Su, Z. G., & Ma, G. H. (2008). Chemical modification and characterization of gigaporous polystyrene microspheres as rapid separation of proteins base supports. *Journal of Polymer Science Part A: Polymer Chemistry*, *46*(17), 5794–5804.

Samani, M. R., Borghei, S. M., Olad, A., & Chaichi, M. J. (2010). Removal of chromium from aqueous solution using polyaniline–polyethylene glycol composite. *Journal of Hazardous Materials*, *184*(1–3), 248–254.

Seppala, J., Littunen, K., Hippi, U., Johansson, L. S., Osterberg, M., Tammelin, T., et al. (2011). Free radical graft copolymerization of nanofibrillated cellulose with acrylic monomers. *Carbohydrate Polymers*, *84*(3), 1039–1047.

Siroky, J., Blackburn, R. S., Bechtold, T., Taylor, J., & White, P. (2011). Alkali treatment of cellulose II fibres and effect on dye sorption. *Carbohydrate Polymers*, *84*(1), 299–307.

Takase, H., & Katoh, N. (1995). Recovery of heavy-metal ion from slurry adsorbent by packed-column of ion-exchange membrane. *Journal of Chemical Engineering of Japan*, *28*(2), 165–170.

Tan, T. W., Zhao, Y., & Kang, J. (2006). Salt-, pH- and temperature-responsive semi-interpenetrating polymer network hydrogel based on poly(aspartic acid) and poly(acrylic acid). *Polymer*, *47*(22), 7702–7710.

Tian, Y., Wu, M., Liu, R. G., Li, Y. X., Wang, D. Q., Tan, J. J., et al. (2011). Electrospun membrane of cellulose acetate for heavy metal ion adsorption in water treatment. *Carbohydrate Polymers*, *83*(2), 743–748.

Ting, Y. P., & Deng, S. B. (2005). Polyethylenimine-modified fungal biomass as a high-capacity biosorbent for Cr(VI) anions: Sorption capacity and uptake mechanisms. *Environmental Science and Technology*, *39*(21), 8490–8496.

Vallapa, N., Wiarachai, O., Thongchul, N., Pan, J. S., Tangpasuthadol, V., Kiatkamjornwong, S., et al. (2011). Enhancing antibacterial activity of chitosan surface by heterogeneous quaternization. *Carbohydrate Polymers*, *83*(2), 868–875.

Wang, J. S., Peng, R. T., Yang, J. H., Liu, Y. C., & Hu, X. J. (2011). Preparation of ethylenediamine-modified magnetic chitosan complex for adsorption of uranyl ions. *Carbohydrate Polymers*, *84*(3), 1169–1175.

Xing, G. X., Zhang, S. F., Ju, B. Z., & Yang, J. Z. (2006). Study on adsorption behavior of crosslinked cationic starch maleate for chromium(VI). *Carbohydrate Polymers*, *66*(2), 246–251.

Xiong, C. H., & Yao, C. P. (2009). Preparation and application of acrylic acid grafted polytetrafluoroethylene fiber as a weak acid cation exchanger for adsorption of Er(III). *Journal of Hazardous Materials*, *170*(2–3), 1125–1132.

Xu, L., Zhao, L., Sun, J., Zhao, Y. H., & Zhai, M. L. (2011). Removal of hazardous metal ions from wastewater by radiation synthesized silica-graft-dimethylaminoethyl methacrylate adsorbent. *Chemical Engineering Journal*, *170*(1), 162–169.

Xu, X., Gao, B. Y., Tan, X., Yue, Q. Y., Zhong, Q. Q., & Li, Q. A. (2011). Characteristics of amine-crosslinked wheat straw and its adsorption mechanisms for phosphate and chromium (VI) removal from aqueous solution. *Carbohydrate Polymers*, *84*(3), 1054–1060.

Zhai, M. L., Wang, M., Xu, L., Peng, J., Li, J. Q., & Wei, G. S. (2009). Adsorption and desorption of Sr(II) ions in the gels based on polysaccharide derivates. *Journal of Hazardous Materials*, *171*(1–3), 820–826.

Zhang, Q., Gao, Y., Zhai, Y. A., Liu, F. Q., & Gao, G. (2008). Synthesis of sesbania gum supported dithiocarbamate chelating resin and studies on its adsorption performance for metal ions. *Carbohydrate Polymers*, *73*(2), 359–363.

Zhang, Z. B., & McCormick, C. L. (1997). Graft copolymerization of cellulose with structopendant unsaturated ester moieties in homogeneous solution. *Journal of Applied Polymer Science*, *66*(2), 307–317.

Zhao, L., & Mitomo, H. (2008). Adsorption of heavy metal ions from aqueous solution onto chitosan entrapped CM-cellulose hydrogels synthesized by irradiation. *Journal of Applied Polymer Science*, *110*(3), 1388–1395.

Zhao, L., Sun, J., Zhao, Y. H., Xu, L., & Zhai, M. L. (2011). Removal of hazardous metal ions from wastewater by radiation synthesized silica-graft-dimethylaminoethyl methacrylate adsorbent. *Chemical Engineering Journal*, *170*(1), 162–169.